

Article

Simulated Impact of Shortened Strings in Commercial and Utility-Scale Photovoltaic Arrays

Ryan M. Smith ¹, Manjunath Matam ² and Hubert Seigneur ^{2,*}¹ Pordis LLC, Austin, TX 78729, USA; ryan.smith@pordis.com² Florida Solar Energy Center, University of Central Florida, Cocoa, FL 32922, USA; manjunath.matam@ucf.edu

* Correspondence: seigneur@ucf.edu

Abstract: The deliberate removal of photovoltaic modules from a string can occur for various reasons encompassing maintenance, measurements, theft, or failure, reducing that string length relative to others when replacement modules are not available and there are not any viable alternative makes and models that could be inserted. This phenomenon, delineated in our prior experimentally validated research, manifests two significant effects: (1) a shift in the ideal maximum power point and (2) the induction of potentially substantial reverse currents in the shortened strings at open-circuit voltage, V_{OC} . However, the scalability and asymptotic limits of these observed behaviors concerning array size remained undetermined. In this study, we elucidate the operational dynamics of such arrays by manipulating two mismatch-contributing variables in simulated arrays of up to 900 strings: the number of removed modules per string (indicative of the level of mismatch, ranging up to 5) and the quantity of shortened strings (1 to 60). Simulation outcomes underscore that mismatch severity impacts array operation more than the proportion of shortened strings. This research delves into the practical ramifications of operating with shortened strings, including implications for low-irradiance operation and the manifestation of deleterious reverse currents (>35A in specific cases), emphasizing the need for careful array configuration for optimal performance and safety in these implementations.

Keywords: photovoltaic string; mismatch; reverse current; modeling; shortened; utility-scale



Citation: Smith, R.M.; Matam, M.; Seigneur, H. Simulated Impact of Shortened Strings in Commercial and Utility-Scale Photovoltaic Arrays. *Energies* **2023**, *16*, 7222. <https://doi.org/10.3390/en16217222>

Academic Editor: Carlo Renno

Received: 1 September 2023

Revised: 17 October 2023

Accepted: 20 October 2023

Published: 24 October 2023



Copyright: © 2023 by the authors. Licensee MDPI, Basel, Switzerland. This article is an open access article distributed under the terms and conditions of the Creative Commons Attribution (CC BY) license (<https://creativecommons.org/licenses/by/4.0/>).

1. Introduction

On a global scale, there is a forecast surge in the installed capacity of photovoltaics, expected to increase by 2400 gigawatts between 2022 and 2027. This uptrend is attributable, in part, to the diminishing cost of PV, with projections indicating that PV will surpass the installed capacity of natural gas and coal by 2026 and 2027, respectively [1]. As the installed capacity of PV proliferates, it is envisaged that PV plants may encounter energy losses, with some attributions to mismatch. Our preceding investigation into the mismatch between module strings extensively reviewed the existing literature, revealing a myriad of causative factors [2]. Diverse mismatch scenarios may encompass electrical faults, unavailability induced by maintenance or component failure, nameplate mismatch, and soiling losses [3]. Analysis of live data collected from 15 PV plants across Spain and Italy shows that the impact of PV plant failures on the energy yield remained at <1% [4]. Simulations have shown that power losses in the PV array due to the nameplate mismatch among the PV modules (mismatch within tolerance limit) is small (0.23%) compared to ohmic losses in cabling (0.5–1.5%) and inverter losses (5–10%) [5]. PV module mismatches as well as PV inverter-related failures contribute around 4.31% to 7.56% of energy losses by making the PV plant unavailable during sun hours [6]. Published reports suggest that PV system output may encounter a reduction of 20 to 25% due to mismatch losses [7]. Mismatch losses in PV plants arise from decisions made during their manufacture or at the design stage, or may manifest during plant operation. Mismatch conditions may arise due to manufacturing tolerances, which are currently typically less than 1% [8], significantly reduced from the previous range of 4–7% [9] reported in earlier generations.

At the design stage, combining modules of different models, manufacturers, and technologies can contribute to mismatch. Discrepancies may manifest in module current due to the series connection of modules or in string voltage due to the parallel connection of strings. In the study by Sahoo et al. [10], an investigation into the mismatch of strings comprising various technologies was carried out. The authors advise against connecting modules of different technologies in the same string, joining modules with the same current rating in series, and configuring modules with the same voltage rating in parallel. da Luz et al. [11] found in their review of systems of various sizes that little attention has been given to persistent mismatch resulting from the interconnection of modules with disparate ratings. While it is conceivable for a design to incorporate multiple module technologies, suppliers, or models, it is generally assumed that most mismatches are unintentional and emerge during plant construction and operation.

Even before the commissioning of a system, in-module faults induced by severe installation and weather conditions (such as cell cracks, interconnect failures, encapsulant issues) start accumulating [12]. Discrepancies in the installation of a PV system, such as variations in module tilt angles and orientation, can lead to mismatch conditions. Additionally, environmental factors such as shading, soiling, snow, or temperature gradient [9] may contribute to mismatch conditions. The impact of partial shading on different PV module technologies was investigated through simulation studies in [13]. Furthermore, in [14], an algorithm was proposed to detect the repeating partial shade events caused by the static structures in the PV array vicinity and avoid the detection of fast moving shades caused by the passing clouds. Here, different technology PV arrays exhibited varying power losses in the presence of mismatched PV modules within the string: thin-film technology PV arrays experienced 0.7% power losses, multicrystalline technology PV arrays experienced 0.6% power losses, and monocrystalline PV arrays experienced 0.4% power losses. Studies on shading-induced mismatch losses in bifacial systems [15] indicate a dependence on factors such as module position within the string, non-uniform albedo, and inter-row spacing. Another study, [16], examined the effect of potential-induced degradation (PID) on 17 modules of a negatively grounded monocrystalline silicon string in a 20 MW PV field, tested indoors under standard conditions. The results revealed a 1.9% mismatch loss in the string, attributed to nonuniform degradation; modules close to the negative terminal degraded faster compared to those near the positive terminal.

Throughout the literature, the consensus is clear: mismatch needs to be detected, quantified, avoided, or mitigated. During operation, voltage mismatch conditions arising from the failure of bypass diodes and homerun voltage drop have been documented in the literature [7,17], and are more prevalent as a system ages. In [18], a machine-learning-based approach was proposed to monitor and detect the mismatch conditions, emphasizing the importance of detecting this type of issue. A survey on the aging of PV modules showed that aging and mismatch are interconnected: different aging of the cells increases the mismatch within a PV module, and thermal mismatches among the PV modules accelerates the nonuniform aging [19]. Furthermore, in [20], their simulation studies proved that large and wide clouds could have a similar impact on different PV array configurations (series-parallel, multi-string, total-cross-tied), but the physical location of the modules and strings adversely impacts the mismatch losses. An improved mathematical model to accurately simulate the PV module behavior and mismatch conditions has been proposed [21], lending weight to the need to understand the impact of mismatch. An optimized Sudoku algorithm was proposed to optimize array mismatch losses [22]. In [23], a matrix based numerical solution was proposed to detect and compute the deep mismatch in the PV array, while in [24], an optimization procedure was proposed to identify the best configuration of PV modules for minimizing mismatch losses. To mitigate mismatch losses, the fixed electrical reconfiguration method proposed in [25] has proven to be effective compared to other configuration methods. Although the modeling and mathematical approaches to understanding and mitigating mismatch have been discussed in the literature, intentional

or unintentional string length mismatch, where a subset of strings is shortened relative to the nominal length, remains an area that requires further in-depth study.

It is understood that modern inverters are capable of managing power point tracking when arrays present multiple peaks in a power–voltage (P-V) curve using modern algorithms and that more advanced design topologies and balance-of-system hardware (i.e., distributed MPP trackers, micro-inverters, or buck–boost converters) may be effective in dealing with temporary or permanent mismatch. Many claims of success in mitigating mismatch issues have been made in the literature and by manufacturers, but many of these claims lack clarity; hardware mitigation strategies are often peppered with statements regarding the power increase gained by the presented solution. Başoğlu [26] found wide variation in the power gains claimed by hardware manufacturers, ranging from ‘no data given’ to 40% with most in the range of 20–25%. However, these gains were not specific regarding the reference condition from which the power increase is claimed. Regardless, the existing body of work, whether theoretical or experimental, does not address utility-scale systems. For example, Başoğlu [26] explains that they expected their review of DMPPT methods to contribute primarily to building-applied and building-integrated implementations, thus not at a utility scale. The work of da Luz [11] only considers a string of four and a string of six modules in their experiment. To the authors’ knowledge, there is no existing published experimental work on this topic at the utility scale. This is understandable as it would require unprecedented access to a power plant. The presented work begins to fill that gap by providing practical ramifications and new results. The limited literature on this topic cautions that one should not assume that what is known at a small scale automatically translates to the utility scale.

While many in the literature have proposed interesting approaches to deal with mismatch issues, realistic costs for the deployment of these approaches at a utility scale must be considered, with a detailed understanding of the potential levelized cost of energy (LCOE) impact. Başoğlu [26], in their treatment of DMPPT methods, concedes that the analysis ignored ‘important criterion such as cost,’ and emphasizes that control methods must be as granular as possible. With high control granularity, these solutions are often not cost-effective at the utility scale, and therefore not realistic nor practical. The presented work manifested from private discussions with a utility-scale plant owner, where string shortening represents a recurring challenge. These facilities are often built with a simple design, at a large scale: series-connected strings of modules, paralleled through combiners and recombiners, ultimately terminating at an inverter with simple perturb and observe (P&O)-type maximum power point tracking; in these plants, no control devices exist at the combiners or recombiners other than protection fuses, and in many plants, multiple strings are combined prior to the protection fuse. An operator may manage module loss by removing the affected modules (thus shortening affected strings), removing impacted strings entirely from the array, or taking the array or sub-array offline until module replacement or array reconfiguration is possible. For the operators of these plants, a simple calculus is presented: identify the least detrimental way to manage module loss, whether temporary or permanent.

For the real-world scenario we present, hardware solutions are not practical solutions; it may be more cost-effective and economical to construct a new PV plant rather than implementing such changes to an existing site (e.g., upgrading to newer central inverters or the replacement of combiners or recombiners with more intelligent distributed control devices). We therefore contend with the presented problem and attempt to inform the operators of plants with similar configurations how module removal may be achieved while limiting energy production impact and avoiding potentially dangerous reverse currents.

Maintenance operations may necessitate the extraction of a module from a string, a procedure conducted periodically for the transportation of modules to indoor laboratories for performance assessments and fault diagnostics [27]. Instances of module removal may also transpire due to theft or in the aftermath of natural disasters, where immediate replacements may encounter impediments related to availability, insurance processes, or warranty

claims [28]. During the construction phase, plant operators typically allocate a finite reserve of modules of the same model in anticipation of substituting missing or damaged modules. Given the continual technological advancements by module manufacturers, the installed module model within a plant may become obsolete or unattainable within a few years post-installation. Consequently, acquiring identical replacement modules from the commercial market becomes challenging in the ensuing years. In cases where immediate replacement modules are unavailable, a prevalent industry practice involves bypassing the removed module(s), resulting in shortened string(s), as acknowledged in the pertinent literature [29]. Although advanced power point tracking algorithms may assist in mitigating the impact of string shortening in some instances, such as in arrays with multiple peaks, the fact remains that an array composed of some proportion of shortened strings will not be capable of generating as much energy as a nominal array under identical irradiance, spectral, and temperature conditions. We therefore do not discuss power point tracking algorithms but focus on array behavior under uniform conditions. As photovoltaic installations have proliferated over the past few decades, the occurrence of string shortening may escalate in these aging systems, potentially precipitating substantial losses due to mismatch and raising safety concerns, particularly in the context of commercial or utility-scale solar plants with hundreds or thousands of strings, aging infrastructure, and simple inverters.

The treatment of mismatch in the existing literature has primarily overlooked the specific case of shortened strings and the consequential effects on current flow. Notably, research efforts have addressed mismatch losses arising from the substitution of PV modules with those of distinct makes or models, as evidenced in [11,30]. In [31], simulations employing a one-diode model (ODM) were conducted, investigating various configurations of unequal-length strings, albeit without considering actual operational conditions. An apparent gap exists in current electrical codes and standards pertaining to PV systems, which lack comprehensive guidance concerning circuit mismatch, over or reverse current protection, and unbalanced operational scenarios in extensive PV installations [32]. Furthermore, experimental investigations into these aspects are constrained by financial considerations and limited resources. While certain studies have documented experimental observations of reverse current flow and the repercussions of blocking diodes, these findings are invariably associated with faults distinct from shortened strings [32]. The nuanced impact of string length mismatch on both nominal and shortened strings needs to be adequately explored and added to the existing body of research.

Preceding research by the authors undertook the experimental validation of simulations, encompassing a basic two-string array [2] configured to represent the use case of simple arrays with P&O-type inverters, and an absence of advanced algorithms and control hardware that was not readily available at the time the arrays of interest were commissioned; that work added to the body of knowledge on mismatch induced by string length variations and aimed to elucidate the repercussions of shortened strings on the overall system output. Included simulations were expanded to encompass arrays of up to 24 strings, focusing on comprehending reverse current flow dynamics. The devised LTspice [33]-based mismatch simulation model, corroborated by empirical validations across diverse mismatch conditions, served to delineate the influence of shortened strings on the array's operating point and the phenomenon of reverse current flow. Despite the insights gained, the confined scale of the simulations precluded definitive conclusions regarding the scalability of observed behaviors concerning array size or the existence of a potential plateau, particularly contingent upon the extent of string length mismatch. In pursuit of resolving these queries, the current study extends the simulations of shortened strings to encompass commercial and small utility-scale systems, scaling up to 900 strings, and provides an exploration of the implications inherent in the observed behaviors.

The subsequent sections of this paper are organized as follows: Section 2 provides an exposition of the simulated PV array, encompassing details on its configuration, dimensions, module specifications, simulated weather conditions, and the simulation software employed. Section 3 is dedicated to the presentation of the simulation results, encompass-

ing diverse PV array sizes, varied irradiance conditions, and an analysis of reverse current flow. In Section 4, an in-depth examination unfolds concerning the impact of shortened strings on arrays of different sizes, the array's maximum power point (MPP) power under varying irradiance conditions, and the occurrence of reverse current flow under open-circuit conditions. Finally, conclusions are presented in Section 5.

2. Materials and Methods

This investigation extends the groundwork established in our antecedent study [2], employing arrays consisting of twelve Jinko Eagle 60 polycrystalline silicon modules (model JKM270PP-60) per string. These series-connected modules are interconnected in parallel and integrated with a grid-tied inverter featuring a single maximum power point tracker. Pertinent parameters from the manufacturer's specification sheet are enumerated in Table 1.

Table 1. Manufacturer specification sheet parameters (STC) for the Jinko Eagle 60 270 W polycrystalline silicon module (JKM270PP-60) [34].

Parameter	Rating
P_{MAX}	270 W _p
V_{MPP}	31.7 V
I_{MPP}	8.52 A
V_{OC}	38.8 V
I_{SC}	9.09 A
Series Fuse	15 A

The methodology for correlating experimental findings with simulations was comprehensively addressed in our prior research and is not reiterated herein. The interested reader is directed to the 'PV plant simulations' reference block within the flow chart (Figure 3 of [2]) for a detailed exposition of this process. The current study is principally concerned with understanding three distinct behaviors: (1) assessing the repercussions of mismatched strings on arrays of varying sizes, (2) analyzing the influence of mismatched strings at the array's maximum power point under diverse irradiance conditions, and (3) scrutinizing the effects of mismatched strings under open-circuit conditions, such as those encountered during array maintenance or in instances where the inverter is experiencing faults.

To comprehend these phenomena, simulations were executed involving the selective disconnection of a subset of modules within the test string, denoted as S_T , effecting the electrical bypass of modules to reduce its module count. This deliberate reduction aimed to induce mismatch conditions between the nominal and test strings. The range of manipulations involved the removal of between zero and five modules from S_T over the course of the investigation. Strings conforming to the standard module count are designated as 'nominal', while those exhibiting mismatched lengths are labeled as ' x -module shortened', with x representing the variance in module count between the nominal and test strings. A visual representation of 1-module shortened strings within an array of n paralleled strings is depicted in Figure 1.

In order to enhance the reproducibility of simulations, the authors prioritized simplicity and accessibility in constructing the simulation model. The model, devised in LTspice—an extensively utilized software for electrical simulations—employs fundamental electrical components to effectively replicate the intricate behavior of photovoltaic arrays. String-level simulations are constructed based on the elemental model components of a photovoltaic string, primarily the module. These simulations were conducted under an experientially relevant operating condition in Cocoa, FL, USA, at 50 °C, encompassing varying irradiance levels ranging from 400 W/m² to 1000 W/m². The thermally static one-diode model is adeptly adjusted to accommodate temperature- and irradiance-dependent parameters using the method delineated by Cubas [35]. Explicit equations for the equiv-

alent circuit parameters are derived from the module manufacturer’s specification sheet parameters under standard test conditions (STC). These module elements are then serially connected and enhanced with fixed resistance elements to accurately represent real-world installation conditions, namely connector resistance (R_{CONN} , measured sample average of 0.013Ω) and home run cable resistance (R_{HR} , determined to be 1.4Ω). For a comprehensive understanding of the technique employed, model development, and validation, refer to our antecedent work [2].

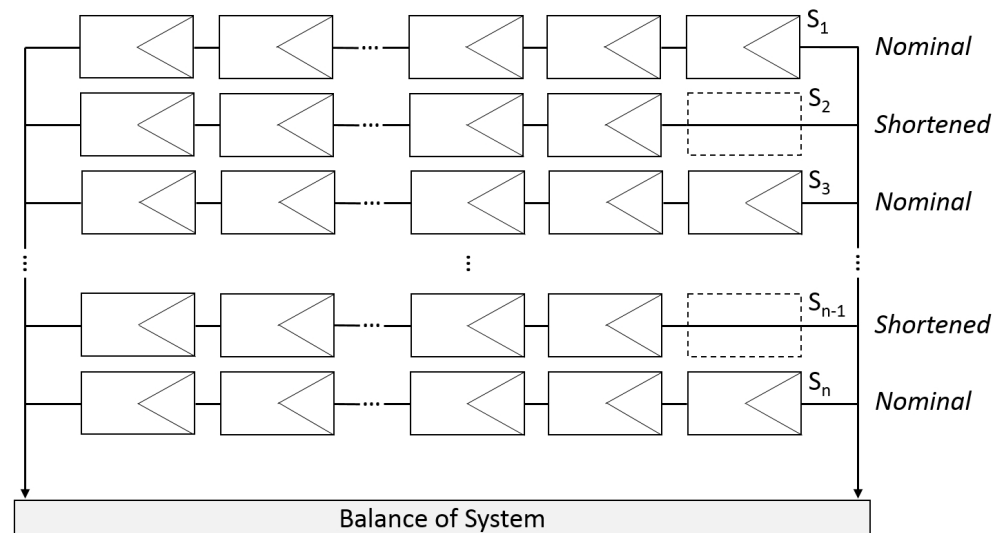


Figure 1. Graphical representation of 1-module shortened ($x = 1$) strings in a parallel array of n strings.

To comprehend the influence of a shortened string on an array, consider the elemental manifestation of a two-string array. Figure 6 in [2] delineates four IV curves elucidating this configuration. One string (S_1) adheres to the nominal module count, while the second string (S_2) is curtailed by three modules. The ‘Nominal Array’ is a reference curve (yellow) characterizing the condition wherein both constituent strings maintain the nominal length. However, when amalgamated into an array, the two-string mismatch array is represented by the red IV curve. Under all circumstances, the nominal length string (black, S_1) and the shortened string (blue, S_2) operate collaboratively to mitigate the mismatch. In the vicinity of I_{SC} , both strings contribute current to the array at nearly equivalent levels. With increasing voltage, the IV curve of the shortened string bends, while the nominal string retains a higher current along the flat segment of the IV curve. Upon reaching a certain point, the IV curve of the shortened string ceases to contribute current to the mismatch array (with S_2 current reaching 0A). At this juncture, all current contribution to the mismatch array is solely derived from the nominal string. As the voltage approaches the open-circuit voltage of the mismatch array, the current produced by the nominal string must be balanced by dissipation in the shortened string. Ultimately, at V_{OC} of the mismatch array, there is a net overall current production of zero, composed of a contribution from the nominal string and equal dissipation within the shortened string. While this scenario provides a comprehensible overview, it constitutes an oversimplification of practical experiences. To discern the impact of more intricate scenarios on array performance and ascertain if trends identified in our prior research extend to larger systems, simulations were conducted for arrays encompassing up to 900 strings (approximately 2.5 MW). Within these simulated arrays, up to 60 strings were intentionally shortened, allowing for an assessment of the array behavior as the proportion of shortened strings varied.

3. Results

Simulations may provide a wealth of data from which trends may be observed. By expanding simulations to 900 strings, the understanding of three key behaviors of how shortened strings impact array performance is enhanced.

3.1. Effect of Array Size

To assess the influence of array size, our simulations were adjusted to (1) vary the total number of paralleled strings within the simulated array, and (2) modify both the number of shortened strings and the severity of shortening (by 1-, 3-, or 5-modules) for each simulated array. In a practical scenario, envision a situation where a fixed number of modules must be removed from an array for measurements or to replace damaged modules, without adding replacements. In such cases, single modules may be removed from multiple strings, or multiple modules may be removed from fewer strings. Figure 2 illustrates this scenario when a total of three (Figure 2a) or sixty (Figure 2b) modules are removed from an array. As irradiance levels impact overall power output, the calculated watt losses must be normalized for meaningful comparison; watt loss is, therefore, converted to equivalent modules by dividing the watt loss by the irradiance-specific P_{MAX} of the nominal module. These normalized values are reported as the number of equivalent modules. This approach ensures that the reported losses are comparable and independent of irradiance levels, providing a clear understanding of the impact of different array sizes and configurations on the system's overall performance.

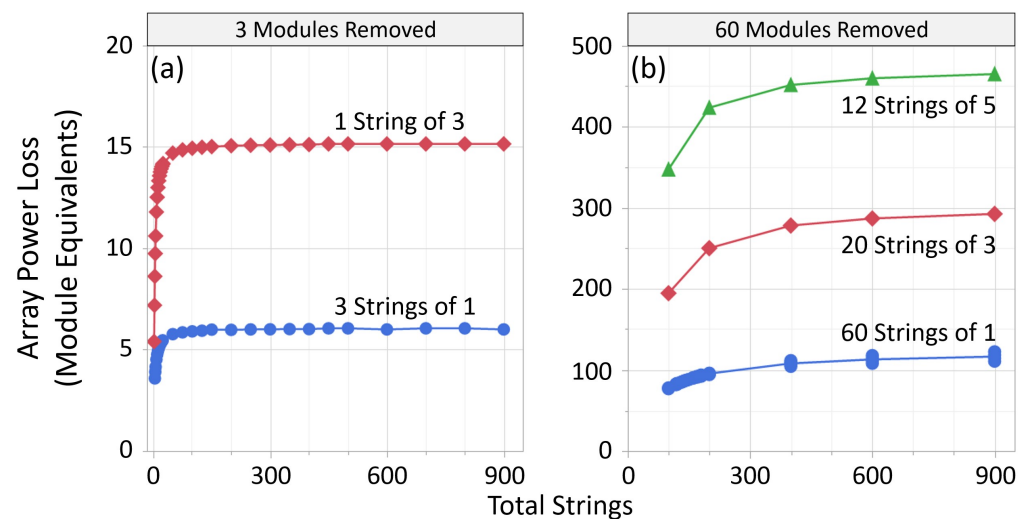


Figure 2. Array power loss in module equivalents at 800 W/m^2 and $50 \text{ }^\circ\text{C}$ for reductions in array size of (a) 3 modules and (b) 60 modules using several string-shortening variations. More extreme levels of shortening for equivalent module removal results in higher relative power losses.

Examining Figure 2a, three modules may be removed from the array either by shortening three strings by one module each or by shortening a single string by three modules. As simulations are extrapolated to arrays consisting of 900 total strings, three crucial observations emerge. Firstly, even the shortening of a single string leads to a greater relative reduction in the array's output than the combined power of the removed modules, regardless of the method of removal. Secondly, the impact on relative power demonstrates a limitation, evident in the flattening of the array power loss curves as the total string count increases. Thirdly, the effect on array power scales with the degree of string-length mismatch. In this illustration, at an array size of 900 strings, the removal of a single module from each of three strings has an impact of 6.004 module equivalents, whereas the removal of three modules from one string (indicating a higher level of mismatch but fewer shortened strings) results in an impact of 15.145 module equivalents.

Expanding the simulation to 60 removed modules from up to 900 total strings, as depicted in Figure 2b, the overall trends persist. The removal of a single module from each of 60 strings has an impact of 114.677 module equivalents, the removal of three modules from each of 20 strings results in an impact of 292.644 module equivalents, and finally, the removal of five modules from each of 12 strings has an impact of 465.031 module equivalents. Irrespective of the quantity of removed modules, the more pronounced the level of

shortening, the more substantial the effect on array output. These observations collectively emphasize the significance of string-length mismatch in influencing the performance of large-scale PV arrays.

3.2. Irradiance Impact on Array Relative Power Loss at P_{MPP}

A 60-module reduction scenario was selected to investigate the impact of irradiance on array power loss in terms of module equivalents; this scenario removes a single module from each of 60 strings and varies only the overall size of the array (up to 900 strings) and the incident irradiance. Module temperature was assumed constant at 50 °C. Shown in Figure 3a, array power loss increases as the total number of strings increases. Notice that for large arrays, the impact in equivalent modules is more substantial at low irradiance than at high irradiance. Indeed, at a 900 string total array size, a loss of 111 module equivalents is experienced at 1000 W/m², while at 400 W/m², the loss increases to a level of 122.6 module equivalents. Furthermore, the module equivalent impact range between low and high irradiance increases with array size.

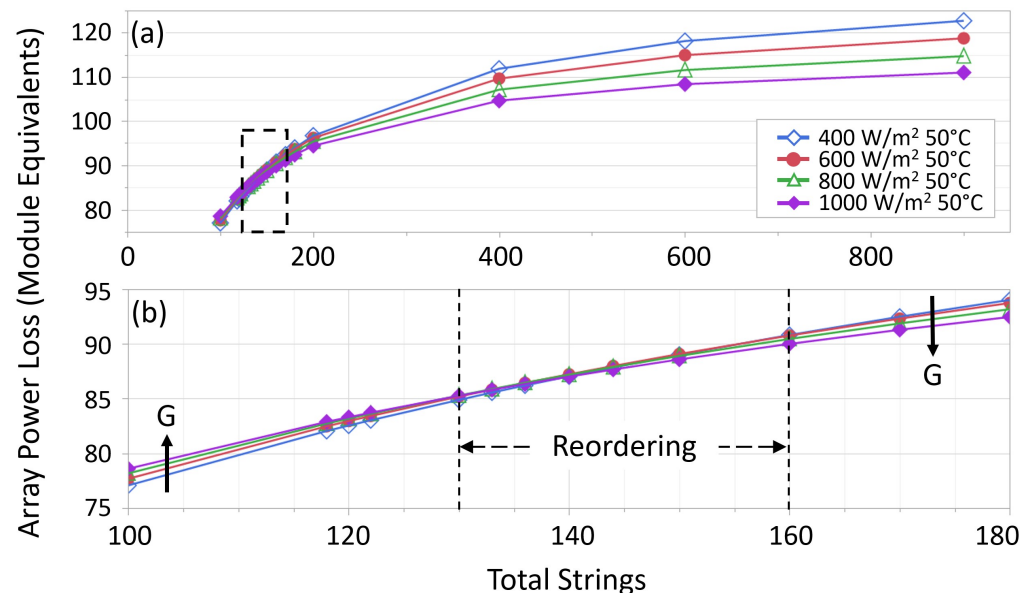


Figure 3. Array power loss in module equivalents as a function of irradiance at 50 °C for a reduction in array size of 60 modules showing (a) the increase in power loss as array size increases, and (b) a magnified section of the full plot showing where the impact of irradiance on power loss re-orders. On the left side of (b), power loss increases as irradiance increases whereas on the right side, power loss increases as irradiance decreases.

However, this relationship reverses when arrays have a low total number of strings, and hence a higher proportion of shortened strings within the array. A section of Figure 3a is expanded into Figure 3b. Above 160 total strings, the impact on array power is as described with the range increasing as array size increases. Below 130 total strings, the relationship is reversed such that power loss increases with increasing irradiance. The power loss range between low and high irradiance conditions is more substantial with small arrays and narrows with increasing array size. Between 130 and 160 total strings, the relationship is not as easily described. Within this region, the power loss range is at a minimum and the irradiance-specific curves shift relative to one another.

3.3. Reverse Current at Open Circuit

Our previous work showed that reverse currents develop in shortened strings at open circuit to a level that correlates to the severity of string shortening. Expanded simulations explore this condition through additional scenarios to determine if the anticipated flattening of the reverse current curves apparent in the initial simulations manifest in larger

arrays. Figure 4 shows several sets of simulations carried out at 800 W/m^2 and $50 \text{ }^\circ\text{C}$. Combinations of six different quantities of shortened strings at three levels of shortening severity (1-, 3-, and 5-module) were explored on arrays of up to 900 total strings.

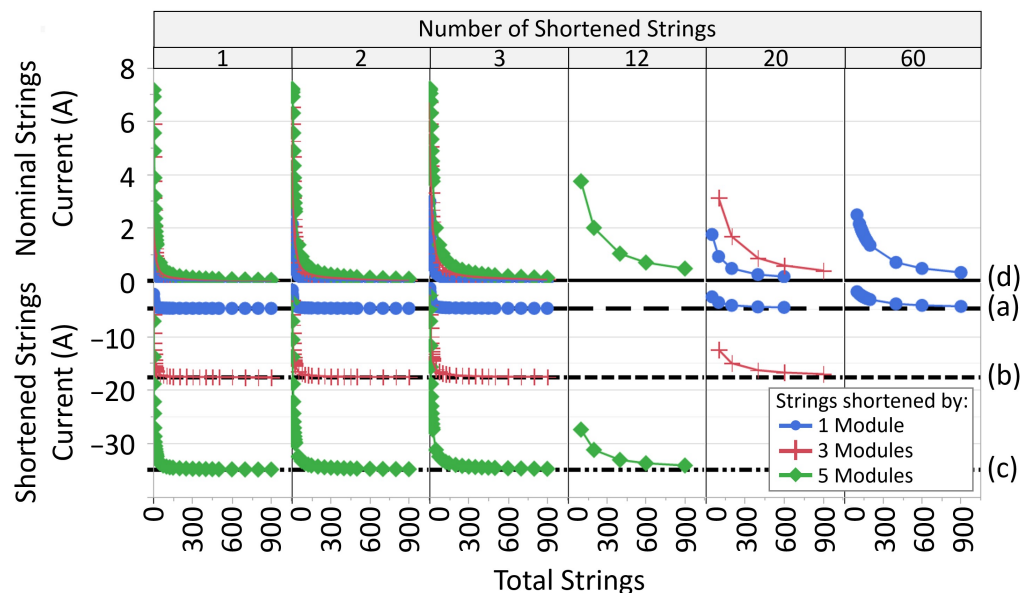


Figure 4. In an open-circuited array, shortened strings exhibit a reverse current (lower half of figure), sourced from nominal strings (upper half of figure). Simulations conducted at 800 W/m^2 and $50 \text{ }^\circ\text{C}$ with varying degrees of string shortening reveal that the reverse current tends to stabilize, reaching a limit determined by the level of mismatch, rather than the number of shortened strings. Specifically: (a) single-module shortened strings self-limit to approximately 4.8 A, (b) three-module shortened strings self-limit to approximately 17.7 A, and (c) five-module shortened strings self-limit to approximately 35 A. As depicted in (d), with an increase in the total number of strings, the contribution of nominal strings to the overall current diminishes to very low levels.

For any number of shortened strings, as the overall size of the array increases, the current generated by the nominal strings decreases and the current consumed within the shortened strings increases. The severity of mismatch (1-, 3-, and 5-module) impacts the magnitude of reverse current with higher severities of mismatch experiencing higher reverse currents, which may exceed the series fuse rating of the modules, thus posing a potential safety concern. The behavior makes intuitive sense as, for a given number of shortened strings, the proportion of nominal strings increases as array size increases and therefore the current generated by each nominal string decreases to achieve balance with the fixed number of shortened strings. As the number of shortened strings increases, the shape of the curve becomes less severe, and the flattening of the curve is less pronounced. Figure 5 overlays these curves for the single module mismatch condition at 800 W/m^2 and $50 \text{ }^\circ\text{C}$. It is expected that the curves for higher numbers of shortened strings would flatten similar to those with low numbers of shortened strings if the simulations were to be carried out to an equivalent multiple of total strings, for example, 54,000 total strings for the 60 shortened strings case (a 900:1 ratio).

Another method of viewing the open-circuit results is to plot the nominal and shortened string currents by the fraction of shortened strings in the array. For instance, one shortened string in an array of 900 strings would have a fraction of 0.0011 and 60 shortened strings in an array of 150 would have a fraction of 0.4. Figure 6 presents the simulations in this manner. Regardless of the severity of the shortening (1-, 3-, or 5-module), the trends remain similar: as the number of shortened strings within a given array increases (hence the shortening fraction increases), the current generated by each nominal string increases, while the current consumed by each shortened string decreases. However, the shape of the curves is related to the severity of mismatch applied to the strings. Single

module shortening displays a linear relationship, while 3- and 5-module shortening shows nonlinear behaviors, which, in the nominal strings, flatten at the I_{SC} of the string at the incident irradiance, while the shortened string currents decrease accordingly to balance with the nominal strings. In all cases, at a shortened fraction of 0.5, the current generated by each nominal string is equal to the current consumed by each shortened string.

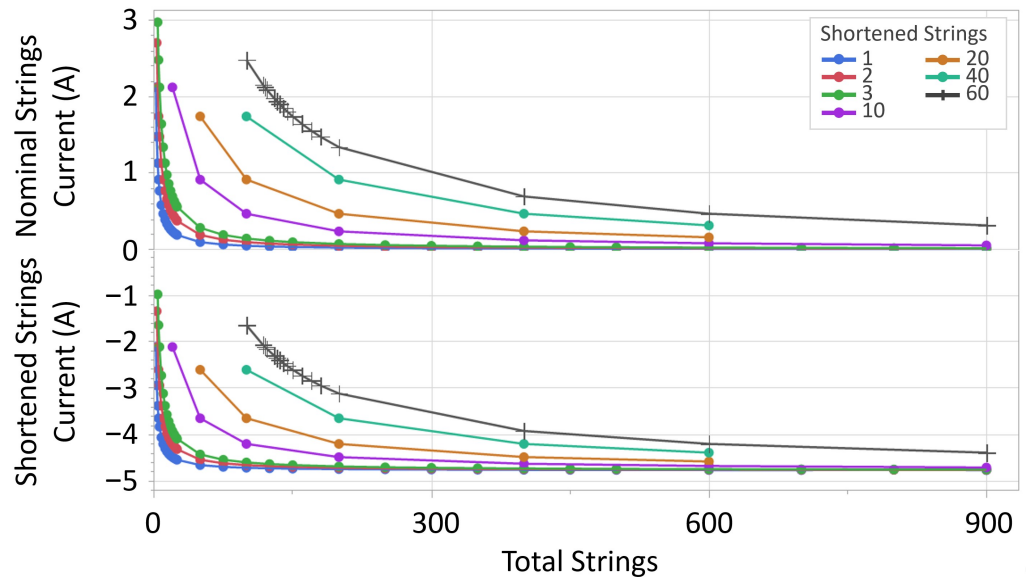


Figure 5. Open-circuit reverse currents at 800 W/m^2 and $50 \text{ }^\circ\text{C}$ for single module shortening showing the impact of increasing quantities of shortened strings.

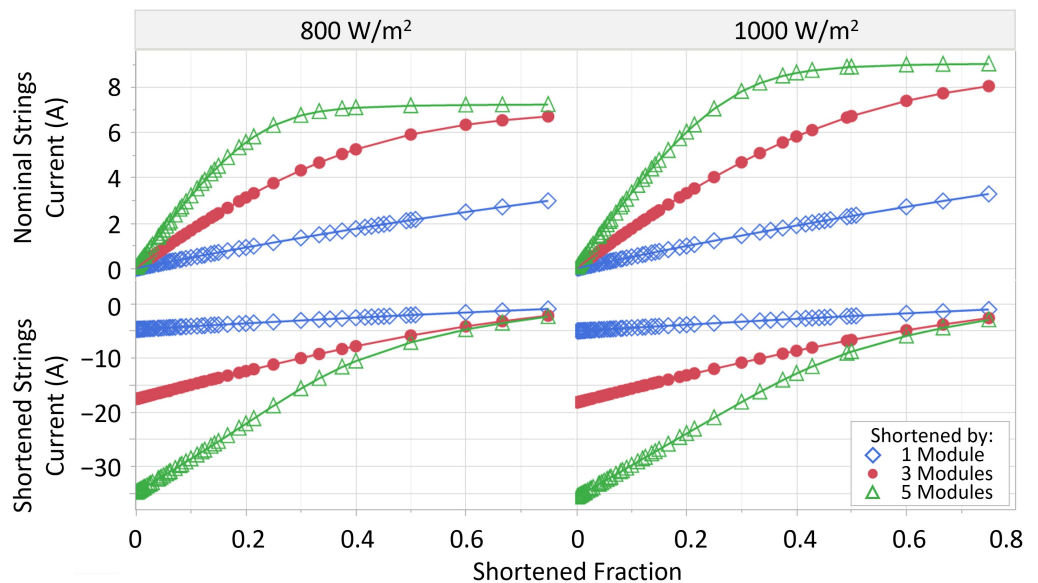


Figure 6. Variation of open-circuit currents in nominal and shortened strings at 800 and 1000 W/m^2 and $50 \text{ }^\circ\text{C}$ across three levels of string shortening, plotted against the fraction of shortened strings within an array.

At an open circuit, the current generated by the nominal string(s) and the reverse current dissipated by the shortened string(s) are in balance only when the number of shortened strings equals the number of nominal strings, a shortened to nominal current ratio of -1.0 . The value is negative since the shortened string current is of the opposite sign to that of the nominal string. When analyzing the shortened to nominal current ratio as a function of the shortened fraction, a single behavior is observed as shown in Figure 7.

All simulations at all irradiances collapse along a single curve, which passes through a ratio of -1.0 when the shortened fraction is 0.5 . Equation (1) is derived from this behavior and calculates the shortened string reverse current given the configuration of the array and the nominal string current; in this equation, I_{SH} is the reverse current flowing into the shortened string(s), I_{NOM} is the current flowing in nominal strings, n_{TOT} is the total number of strings, and, n_{SH} is the number of shortened strings.

$$I_{SH} = -1 * I_{NOM} * \left(\frac{n_{TOT} - n_{SH}}{n_{SH}} \right) \quad (1)$$

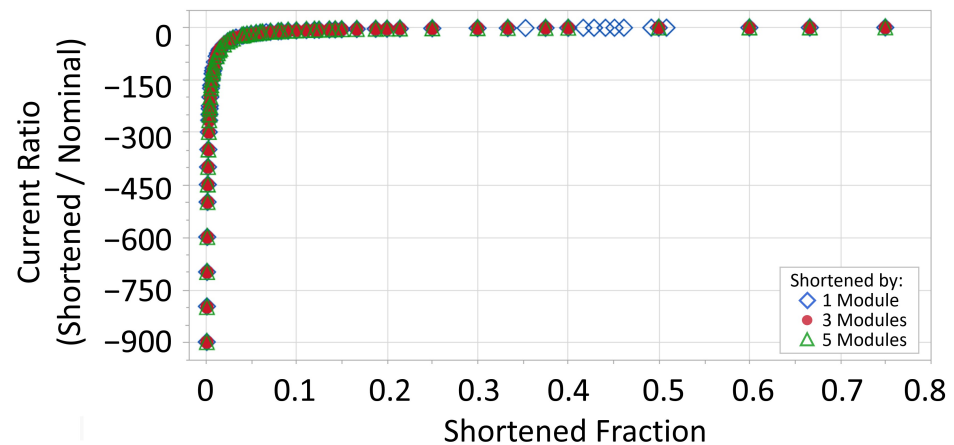


Figure 7. The relationship between the ratio of shortened to nominal string current and the fraction of shortened strings within an array. A unified curve is observed, encompassing all levels of shortening and irradiance conditions.

4. Discussion

The simulations undertaken in this study contribute to the comprehension of array performance in the context of string mismatch resulting from string shortening, primarily for the aging arrays for which string shortening is more probable: basic paralleled string arrays lacking advanced control hardware and modern maximum power point tracking algorithms. Our investigation centered on three principal areas, shedding light on these aspects of array behavior:

1. **Array Size Dynamics:** Delving into the impact of mismatched strings on arrays of diverse sizes, our simulations provide insights into the scalability of these effects across arrays, thereby addressing a critical dimension in array operation.
2. **Maximum Power Point Considerations:** A key facet of our exploration involved assessing the impact of mismatched strings at the array's maximum power point, under varying irradiance conditions. This analysis unravels the intricate interplay between string mismatch and array performance at critical operating points.
3. **Open Circuit Examination:** We extended our scrutiny to evaluate the repercussions of mismatched strings at open circuit conditions. This dimension of our investigation aimed to uncover potential challenges arising during specific operational scenarios, such as maintenance activities or inverter faults.

The multifaceted nature of our study allows for a comprehensive discussion of the observed behaviors, their interdependencies, and implications for the operation of the described category of photovoltaic arrays.

The investigation into the interplay of array size and string shortening reveals intriguing dynamics. As array size scales up, the introduction of additional shortened strings exhibits a limited impact on array power loss. This limiting behavior, however, is intricately linked to the severity of mismatch, denoted by the 1-, 3-, or 5-module variations between strings.

A pivotal metric for gauging this impact on array power is the concept of equivalent modules, calculated by dividing the total array power loss in watts by the nominal module power at the designated irradiance. Across scenarios, it is evident that any level of mismatch induced by string shortening exerts a more significant module equivalent impact on array output than the cumulative power of the removed modules. Practical implications come to the fore when the module equivalent impact surpasses the loss incurred by simply removing the affected strings from production.

Illustratively, at 800 W/m^2 and $50 \text{ }^\circ\text{C}$, shortening one string by one module in a 900-string array yields an impact of 2.02 module equivalents. Conversely, disconnecting that string would result in a higher impact of 12 module equivalents. Operationally, it therefore remains advantageous to retain the string in production. Scaling up to 60 strings with single-module shortening intensifies the impact to 114.7 module equivalents, yet decommissioning all 60 strings would lead to a more substantial decrease of 720 module equivalents, reinforcing the operational benefit of retention for single module shortening.

The dynamics become more nuanced when considering scenarios involving the increased severity of string shortening. For instance, when 20 strings are reduced by three modules each, totaling 60 modules removed, the impact on a 900-string array is 292.6 module equivalents. However, disconnecting all 20 of those strings would result in a more modest impact of 240 module equivalents, making the latter option more beneficial from a power production perspective. This pattern is further accentuated when 12 strings undergo a five-module reduction each, extracting 60 modules from the 900-string array. In this case, the array's output is significantly reduced by 465 module equivalents, whereas disconnecting the 12 strings yields a more conservative impact of 144 module equivalents, underscoring the nuanced considerations in optimizing array performance under varying string shortening scenarios.

The influence of irradiance on mismatch arrays is contingent upon the array shortened fraction. In the current work, with a focus on low shortened fractions (below 0.375), it is observed that the module equivalent impact is more pronounced at low irradiance compared to high irradiance. Conversely, for high shortened fractions (above 0.4), the reverse behavior is observed. In practical scenarios, string shortening is more likely in arrays with a substantial total number of strings, resulting in a small shortened fraction. In such cases, operators should recognize that the impact of a string shortening mismatch is particularly notable at low irradiance, and the expected reduction in array power output during periods of low irradiance will be further diminished due to string shortening.

Concerns arise regarding reverse currents in shortened strings during open circuit operation at high irradiance, such as when a plant undergoes maintenance or an inverter experiences a fault. In such instances, the array self-balances, ensuring that the combined current generation from nominal strings and current dissipation in shortened strings equates to zero. Simulations reveal that the level of reverse current stabilizes with increasing array size, with a magnitude contingent on the severity of mismatch between nominal and shortened strings. More severe mismatches result in higher reverse currents. In simulations, single-module shortened string reverse currents remain below 4.78 A, well within the 15 A series fuse rating of the modules, suggesting no immediate safety concerns; however, potential reliability or degradation impacts remain uncertain. Conversely, 3- and 5-module mismatches yield reverse currents of approximately 17.7 A and 35 A, respectively, surpassing the series fuse rating. When strings are paralleled before a combiner box fuse, which the authors have confirmed to exist in utility-scale arrays, the possibility arises for a shortened string to operate above the series fuse current rating without triggering the protection device. Operating under these conditions raises substantial safety and likely reliability concerns. Our previous research demonstrated that string-level blocking diodes effectively mitigate reverse currents, but their practicality and reliability for large-scale systems warrant further consideration. This study highlights the importance of addressing safety and reliability implications associated with reverse currents in large-scale PV systems undergoing string shortening.

For the behaviors to have utility in system design and operation, a model must be developed that predicts the mismatch string current for any array configuration and module type. This is part of the authors' future efforts and the simulation work presented provides the basis for these efforts.

5. Conclusions

The presented work compiles the results of simulations of shortened strings in simple arrays consisting of paralleled strings of series-connected modules that feed an inverter using the basic perturb and observe type of maximum power point tracking. Practical application of the conclusions is relevant for commercial and utility-scale plants where cost and scale requires design simplicity and therefore lack any sort of distributed control or some of the more advanced maximum power point tracking capabilities. The insights derived from this research offer valuable guidance to plant operators, providing strategies for managing instances of shortened strings arising from maintenance, measurements, module failures, or theft.

Simulations affirm the importance of limiting string shortening to single modules, as increasing the severity of shortening by removing additional modules substantially impacts relative power loss, consistently surpassing the combined power of the removed modules. Key considerations and practical implications emerge:

1. **Severity Dictates Impact:** The impact of string shortening at a given severity is influenced by the fraction of impacted strings in the array.
2. **Practical Implications:** Small shortened fractions, likely under real-world conditions, should be carefully managed, with operators noting that the relative impact is more pronounced at low irradiance than at high irradiance.
3. **Variable Power Output:** System power output may exhibit more pronounced dips during cloudy skies, sunrise, or sunset, compared to predictions from a nominal array model at a given irradiance.
4. **Reverse Current Concerns:** Concerns regarding reverse currents are notable when an array is at open circuit and elevated irradiance, potentially during inverter shutdowns for maintenance or faults. Single-module shortening presents no significant reverse current concerns, while 3- and 5-module shortened string configurations may exceed series fuse ratings, warranting attention to safety and reliability. Strings paralleled prior to protection fuses require special consideration of reverse currents.

This comprehensive investigation provides valuable insights for optimizing the operational management of basic photovoltaic arrays with the existence of shortened strings, emphasizing the need for cautious consideration of string shortening practices and anticipating potential challenges associated with varying degrees of severity.

Author Contributions: Methodology, R.M.S., M.M. and H.S.; investigation, R.M.S. and M.M.; software, R.M.S.; formal analysis, R.M.S.; visualization, R.M.S.; writing—original draft preparation, R.M.S., M.M. and H.S.; writing—review and editing, R.M.S., M.M. and H.S.; funding acquisition, H.S.; project administration, H.S.; supervision, H.S. All authors have read and agreed to the published version of the manuscript.

Funding: This material is based upon work funded by the U.S. Department of Energy's Solar Energy Technologies Office Award Number DE-EE-0008157. The opinions, findings, and conclusions stated herein are those of the authors and do not necessarily reflect those of the U.S. Department of Energy.

Data Availability Statement: Model data are available by contacting the corresponding author.

Conflicts of Interest: The authors declare no conflict of interest.

References

1. International Energy Agency. *Renewables 2022*; Technical Report; International Energy Agency: Paris, France, 2022.
2. Smith, R.M.; Matam, M.; Seigneur, H. Mismatch losses in a PV system due to shortened strings. *Energy Convers. Manag.* **2021**, *250*, 114891. [[CrossRef](#)]
3. Ilse, K.; Micheli, L.; Figgis, B.W.; Lange, K.; Daßler, D.; Hanifi, H.; Wolfertstetter, F.; Naumann, V.; Hagendorf, C.; Gottschalg, R.; et al. Techno-economic assessment of soiling losses and mitigation strategies for solar power generation. *Joule* **2019**, *3*, 2303–2321. [[CrossRef](#)]
4. Lillo-Bravo, I.; González-Martínez, P.; Larrañeta, M.; Guasumba-Codena, J. Impact of energy losses due to failures on photovoltaic plant energy balance. *Energies* **2018**, *11*, 363. [[CrossRef](#)]
5. Lorente, D.G.; Pedrazzi, S.; Zini, G.; Dalla Rosa, A.; Tartarini, P. Mismatch losses in PV power plants. *Sol. Energy* **2014**, *100*, 42–49. [[CrossRef](#)]
6. Kumar, N.M.; Dasari, S.; Reddy, J.B. Availability factor of a PV power plant: Evaluation based on generation and inverter running periods. *Energy Procedia* **2018**, *147*, 71–77. [[CrossRef](#)]
7. Shin, W.G.; Lim, J.R.; Kang, G.H.; Ju, Y.C.; Hwang, H.M.; Ko, S.W. Current flow analysis of PV arrays under voltage mismatch conditions and an inverter failure. *Appl. Sci.* **2019**, *9*, 5163. [[CrossRef](#)]
8. Chaudhari, C.; Kimball, G.M.; Hickey, R.; Bourne, B. Quantification of System-Level Mismatch Losses using PVMismatch. In Proceedings of the 2018 IEEE 7th World Conference on Photovoltaic Energy Conversion (WCPEC) (A Joint Conference of 45th IEEE PVSC, 28th PVSEC 34th EU PVSEC), Waikoloa Village, HI, USA, 10–15 June 2018; pp. 3626–3629. [[CrossRef](#)]
9. Mansur, A.A.; Amin, M.R.; Islam, K.K. Performance comparison of mismatch power loss minimization techniques in series-parallel PV array configurations. *Energies* **2019**, *12*, 874. [[CrossRef](#)]
10. Sahoo, S.K.; Shah, M.; Dawlatzai, N.A.; Ann Jerin Amalorpavaraj, R. Assessment of mismatching in series and parallel connection of the PV modules of different technologies and electrical parameters. In Proceedings of the 2020 International Conference on Computer Communication and Informatics (ICCCI), Coimbatore, India, 22–24 January 2020; pp. 1–5.
11. Meira Amaral da Luz, C.; Moreira Vicente, E.; Lessa Tofoli, F.; Roberto Ribeiro, E. Differential power processing architecture to increase energy harvesting of photovoltaic systems under permanent mismatch. *Sol. Energy* **2023**, *263*, 111940. [[CrossRef](#)]
12. Eskandari, A.; Milimonfared, J.; Aghaei, M. Line-line fault detection and classification for photovoltaic systems using ensemble learning model based on I-V characteristics. *Sol. Energy* **2020**, *211*, 354–365. [[CrossRef](#)]
13. Wang, Z.; Zhou, N.; Gong, L.; Jiang, M. Quantitative estimation of mismatch losses in photovoltaic arrays under partial shading conditions. *Optik* **2020**, *203*, 163950. [[CrossRef](#)]
14. Matam, M.; Barry, V.R. Improved performance of Dynamic Photovoltaic Array under repeating shade conditions. *Energy Convers. Manag.* **2018**, *168*, 639–650. [[CrossRef](#)]
15. Deline, C.; Ayala Pelaez, S.; MacAlpine, S.; Olalla, C. Estimating and parameterizing mismatch power loss in bifacial photovoltaic systems. *Prog. Photovolt. Res. Appl.* **2020**, *28*, 691–703. [[CrossRef](#)]
16. Wang, H.; Cheng, X.; Yang, H.; He, W.; Chen, Z.; Xu, L.; Song, D. Potential-induced degradation: Recombination behavior, temperature coefficients and mismatch losses in crystalline silicon photovoltaic power plant. *Sol. Energy* **2019**, *188*, 258–264. [[CrossRef](#)]
17. Lee, C.G.; Shin, W.G.; Lim, J.R.; Kang, G.H.; Ju, Y.C.; Hwang, H.M.; Chang, H.S.; Ko, S.W. Analysis of electrical and thermal characteristics of PV array under mismatching conditions caused by partial shading and short circuit failure of bypass diodes. *Energy* **2021**, *218*, 119480.
18. Liu, G.; Yu, W.; Zhu, L. Experiment-based supervised learning approach toward condition monitoring of PV array mismatch. *IET Gener. Transm. Distrib.* **2019**, *13*, 1014–1024. [[CrossRef](#)]
19. Manganiello, P.; Balato, M.; Vitelli, M. A Survey on Mismatching and Aging of PV Modules: The Closed Loop. *IEEE Trans. Ind. Electron.* **2015**, *62*, 7276–7286. [[CrossRef](#)]
20. Lappalainen, K.; Valkealahti, S. Effects of irradiance transition characteristics on the mismatch losses of different electrical PV array configurations. *IET Renew. Power Gener.* **2017**, *11*, 248–254. [[CrossRef](#)]
21. Bastidas, J.; Franco, E.; Petrone, G.; Ramos-Paja, C.; Spagnuolo, G. A model of photovoltaic fields in mismatching conditions featuring an improved calculation speed. *Electr. Power Syst. Res.* **2013**, *96*, 81–90. [[CrossRef](#)]
22. Potnuru, S.R.; Pattabiraman, D.; Ganesan, S.I.; Chilakapati, N. Positioning of PV panels for reduction in line losses and mismatch losses in PV array. *Renew. Energy* **2015**, *78*, 264–275. [[CrossRef](#)]
23. Orozco-Gutierrez, M.; Ramirez-Scarpetta, J.; Spagnuolo, G.; Ramos-Paja, C. A technique for mismatched PV array simulation. *Renew. Energy* **2013**, *55*, 417–427. [[CrossRef](#)]
24. Orozco-Gutierrez, M.L.; Spagnuolo, G.; Ramirez-Scarpetta, J.M.; Petrone, G.; Ramos-Paja, C.A. Optimized Configuration of Mismatched Photovoltaic Arrays. *IEEE J. Photovolt.* **2016**, *6*, 1210–1220. [[CrossRef](#)]
25. Satpathy, P.R.; Sharma, R. Power and mismatch losses mitigation by a fixed electrical reconfiguration technique for partially shaded photovoltaic arrays. *Energy Convers. Manag.* **2019**, *192*, 52–70. [[CrossRef](#)]
26. Başoğlu, M.E. Comprehensive review on distributed maximum power point tracking: Submodule level and module level MPPT strategies. *Sol. Energy* **2022**, *241*, 85–108. [[CrossRef](#)]
27. Manajit, S.; Aron, H.; Gueymard, C.; Wilbert, S.; Renne, D. *Best Practices Handbook for the Collection and Use of Solar Resource Data for Solar Energy Applications*; Technical Report; National Renewable Energy Lab. (NREL): Golden, CO, USA, 2017. [[CrossRef](#)]

28. National Renewable Energy Laboratory; Sandia National Laboratory; SunSpec Alliance; The SunShot National Laboratory Multiyear Partnership (SuNLaMP) PV O&M Best Practices Working Group. *Best Practices for Operation and Maintenance of Photovoltaic and Energy Storage Systems*; Technical Report; National Renewable Energy Lab. (NREL): Golden, CO, USA, 2018. [[CrossRef](#)]
29. Ishii, T.; Choi, S.; Sato, R.; Chiba, Y.; Masuda, A. Potential-induced degradation in photovoltaic modules composed of interdigitated back contact solar cells in photovoltaic systems under actual operating conditions. *Prog. Photovolt. Res. Appl.* **2020**, *28*, 1322–1332. [[CrossRef](#)]
30. Fregosi, D.; Libby, C.; Smith, M.; Bolen, M. Guidance on PV module replacement. In Proceedings of the 2020 47th IEEE Photovoltaic Specialists Conference (PVSC), Calgary, AB, Canada, 15 June–21 August 2020; pp. 1581–1583. [[CrossRef](#)]
31. Wurster, T.S.; Schubert, M.B. Mismatch loss in photovoltaic systems. *Sol. Energy* **2014**, *105*, 505–511. [[CrossRef](#)]
32. Vargas, J.P.; Goss, B.; Gottschalg, R. Large scale PV systems under non-uniform and fault conditions. *Sol. Energy* **2015**, *116*, 303–313. [[CrossRef](#)]
33. Analog Devices. LTspice Simulator. 2023. Available online: <https://www.analog.com/en/design-center/design-tools-and-calculators/ltspice-simulator.html> (accessed on 30 August 2023).
34. Jinko Solar. Eagle 60 Datasheet. 2015. Available online: <https://jinkosolar.us/wp-content/uploads/2019/03/US-Eagle-60-255-270w.pdf> (accessed on 30 August 2023).
35. Cubas, J.; Pindado, S.; Manuel, C.D. Explicit Expressions for Solar Panel Equivalent Circuit Parameters Based on Analytical Formulation and the Lambert W-Function. *Energies* **2014**, *7*, 4098–4115. [[CrossRef](#)]

Disclaimer/Publisher’s Note: The statements, opinions and data contained in all publications are solely those of the individual author(s) and contributor(s) and not of MDPI and/or the editor(s). MDPI and/or the editor(s) disclaim responsibility for any injury to people or property resulting from any ideas, methods, instructions or products referred to in the content.